

Bipartite Graph Diffusion Model for Human Interaction Generation

Baptiste Chopin¹, Hao Tang², Mohamed Daoudi^{3,4}

¹Univ. Lille, CNRS, Centrale Lille, UMR 9189 CRISAL, F-59000 Lille, France

²Computer Vision Lab, ETH Zurich, Switzerland

³IMT Nord Europe, Institut Mines-Télécom, Univ. Lille, Centre for Digital Systems, F-59000 Lille, France

⁴Univ. Lille, CNRS, Centrale Lille, Institut Mines-Télécom, UMR 9189 CRISAL, F-59000 Lille, France
baptiste.chopin@univ-lille.fr, hao.tang@vision.ee.ethz.ch, mohamed.daoudi@imt-nord-europe.fr

Abstract

The generation of natural human motion interactions is a hot topic in computer vision and computer animation. It is a challenging task due to the diversity of possible human motion interactions. Diffusion models, which have already shown remarkable generative capabilities in other domains, are a good candidate for this task. In this paper, we introduce a novel bipartite graph diffusion method (BiGraphDiff) to generate human motion interactions between two persons. Specifically, bipartite node sets are constructed to model the inherent geometric constraints between skeleton nodes during interactions. The interaction graph diffusion model is transformer-based, combining some state-of-the-art motion methods. We show that the proposed achieves new state-of-the-art results on leading benchmarks for the human interaction generation task.

1 Introduction

Modeling dynamics of human motion interaction is at the core of many applications in computer vision and computer graphics. Most works on human motion generation ignore human interactions and focus instead on the generation of actions of a single person [Zhang *et al.*, 2022; Tseng *et al.*, 2022]. In this paper, we explore the problem of generating 3D human motion interaction. What makes interaction generation challenging are the non-linearity of human motion interaction and the diversity of the interaction between humans. Several questions arise to tackle these challenges. How to represent the interaction between humans? How to model motion and generate diverse motion interaction? To solve the first question, we propose to represent the skeleton interaction by using a bipartite graph [Tang *et al.*, 2020]. The main goal of the bipartite graph is to capture the relations between humans represented by skeletons. To solve the second question, the motion interaction generation is formulated as a reverse diffusion process. Overall, our contributions are summarized as follows:

- We propose the first Bipartite graph denoising diffusion model (BiGraphDiff) for human interaction gener-

ation. Our BiGraphDiff is able to generate motion interaction in a stochastic way, naturally leading to high diversity, and is able to generate very long motion sequences (>1000 frames).

- BiGraphDiff is a denoising diffusion process that learns not only the denoising of the motion, but also it learns a Bipartite graph. The aim of Bipartite graph is to capture the relations between the two persons.
- BiGraphDiff achieves state-of-the-art quantitatively and qualitatively in action interaction and dance tasks. A user study shows that the generated sequences are better qualitatively than the sequences generated by state-of-the-art methods.

2 Related Work

We discuss the relevant literature from two perspectives, namely, previous methods of Human interaction motion synthesis and the literature on diffusion models.

Human Interaction Motion Generation. Recently there has been an increase in motion generation based on different modalities, [Yin *et al.*, 2021] use control signals such as the global trajectory of the person to generate human motion in long-term horizons while [Ahuja *et al.*, 2020] and [Habibie *et al.*, 2021] generate motion based on speech audio. Meanwhile, others use only knowledge of the past motion which allows them to work in real-time but on shorter motion [Martinez *et al.*, 2017; Cui *et al.*, 2020; Sofianos *et al.*, 2021]. More recently, several works have been dedicated to human pose and motion generation from text or action labels, as well as its reciprocal task [Guo *et al.*, 2022; Lucas *et al.*, 2022]. These papers focus only on one person, while our approach is dedicated to the generation of two-person interactions. [Baruah and Banerjee, 2020] propose a multimodal variational recurrent neural network to predict the future motion of both participants in an interaction based on pasts sequences of motion. In contrast, we propose to generate human interaction between two persons.

Generative Diffusion Models. Diffusion models [Sohl-Dickstein *et al.*, 2015; Ho *et al.*, 2020a] have shown great promise in terms of generative modeling by showing impressive results in synthesis applications ranging from image generation [Harvey *et al.*, 2022], audio-drive motion synthesis [Alexanderson *et al.*, 2022], molecule generation [Hooge-

boom *et al.*, 2022], to text-driven motion generation [Saharia *et al.*, 2022]. More recently, some concurrent work in the field of text-to-motion introduces a diffusion-based method for generating text-conditioned motion. For example, [Zhang *et al.*, 2022] propose MotionDiffuse, a diffusion model-based text-driven motion generation framework. [Tseng *et al.*, 2022] propose EDGE, a method for generating editable dances that is able to create a realistic dance while remaining faithful to the original music. [Dabral *et al.*, 2022] introduce MoFusion, a denoising-diffusion-based framework for high-quality conditional human motion synthesis that can generate long and temporally plausible motions conditioned based on music or text. Despite achieving impressive performance, these methods use a diffusion-based method for generating the motion of only one person. In contrast, our proposed method BiGraphDiff proposes to generate the interaction between two persons and propose to learn a bipartite graph during the diffusion process. In addition, BiGraphDiff is applied for both text-to-motion and text-to-dance, and it is able to generate a long sequence of dance motion.

3 Bipartite Graph Diffusion Model

3.1 Framework Overview

Our goal is to generate a human motion interaction $x^{1:N}$ given an arbitrary condition c . Let us consider $x^{1:N} = \{x^1, \dots, x^N\}$ an arbitrary sequence of joints that compose the two skeletons, $x^i \in \mathbb{R}^{k \times 3 \times 2}$, where k is the number of joints. The motion generation is formulated as a reverse diffusion process that requires sampling a random noise $x_t^{1:N}$ from noise distribution to generate a motion sequence. While the forward process requires successively corrupting the motion sequence $x_t^{1:N}$ by adding the noise to the motion sequence for T timesteps in Markov fashion. We propose Transformers to learn the denoising function and a bipartite graph to represent the relationship between the joints of the skeleton. The proposed Transformer learns not only the denoising function but also the bipartite graph. See Fig. 1 for an overview.

3.2 Diffusion for Motion Generation

The diffusion model consists of two separate processes called forward diffusion and reverse diffusion. During the forward diffusion process, we add to real data a small amount of Gaussian noise repeatedly until the data becomes Gaussian noise. Formally, the forward process on a real sample from a real data distribution $x_0^{1:N} \sim q(x^{1:N})$ consists in a Markov chain that gradually adds noise following a variance schedule β_t to obtain the posterior $q(x_{1:T}^{1:N} | x_0^{1:N})$ with $x_1^{1:N}$ to $x_T^{1:N}$ the latent data:

$$\begin{aligned} q(x_{1:T}^{1:N} | x_0^{1:N}) &:= \prod_{t=1}^T q(x_t^{1:N} | x_{t-1}^{1:N}), \\ q(x_t^{1:N} | x_{t-1}^{1:N}) &:= \mathcal{N}(x_t^{1:N}; \sqrt{1 - \beta_t} x_{t-1}^{1:N}, \beta_t \mathbf{I}). \end{aligned} \quad (1)$$

Eventually with $T \rightarrow +\infty$ the distribution will be close to $\mathcal{N}(\mathbf{0}, \mathbf{I})$. This formulation implies that the forward process is recursive but this can be avoided by using [Ho *et al.*, 2020b] formulation:

$$q(x_t^{1:N} | x_0^{1:N}) = \sqrt{\alpha_t} x_0^{1:N} + \sqrt{1 - \alpha_t} \epsilon, \epsilon \sim \mathcal{N}(\mathbf{0}, \mathbf{I}), \quad (2)$$

with $\bar{\alpha}_t = \prod_{i=0}^t \alpha_i$ and $\alpha_t = 1 - \beta_t$. With this formulation, we can sample a noise ϵ and directly generate any $x_t^{1:N}$. Forward diffusion does not require any training but only gradually adds noise to real data. To generate motions, we need to be able to obtain clean data from noisy data to reverse the forward process.

The reverse diffusion process, $p_\theta(x_{0:T}^{1:N})$, is a Markov chain that eliminates the noise from $x_T^{1:N}$ recursively until we obtain $x_0^{1:N}$. With $p(x_T^{1:N}) = \mathcal{N}(x_T^{1:N}; \mathbf{0}, \mathbf{I})$:

$$\begin{aligned} p(x_{0:T}^{1:N}) &:= p(x_T^{1:N}) \prod_{t=1}^T p_\theta(x_{t-1}^{1:N} | x_t^{1:N}), \\ p_\theta(x_{t-1}^{1:N} | x_t^{1:N}) &:= \mathcal{N}(x_{t-1}^{1:N}; \mu_\theta(x_t^{1:N}, t, c), \Sigma_\theta(x_t^{1:N}, t, c)). \end{aligned} \quad (3)$$

During the denoising process the goal is to estimate $\mu_\theta(x_t^{1:N}, t, c)$ and $\Sigma_\theta(x_t^{1:N}, t, c)$. However, if we use Eq. (2) formulation and [Ho *et al.*, 2020b] method then we can set $\Sigma_\theta(x_t^{1:N}, t, c) = \sigma_t^2 \mathbf{I}$ with σ_t a constant and replace $\mu_\theta(x_t^{1:N}, t, c)$ as follow:

$$\mu_\theta(x_t^{1:N}, t, c) = \frac{1}{\sqrt{\alpha_t}} (x_t^{1:N} - \frac{1 - \alpha_t}{\sqrt{1 - \alpha_t}} \epsilon_\theta(x_t^{1:N}, t, c)), \quad (4)$$

this means that we only need to estimate $\epsilon_\theta(x_t^{1:N}, t, c)$ to be able to denoise the latent data since we can recover $x_{t-1}^{1:N}$ using:

$$x_{t-1}^{1:N} = \frac{1}{\sqrt{\alpha_t}} (x_t^{1:N} - \frac{1 - \alpha_t}{\sqrt{1 - \alpha_t}} \epsilon_\theta(x_t^{1:N}, t, c)) + \sigma_t \gamma, \quad (5)$$

with $\gamma \sim \mathcal{N}(\mathbf{0}, \mathbf{I})$. In our model we set $\sigma_t = \log(\beta_t \frac{1 - \alpha_{t-1}}{1 - \alpha_t})$ following [Ho *et al.*, 2020b] recommendation. To estimate $\epsilon_\theta(x_t^{1:N}, t, c)$ we will train a Bipartite Graph Interaction Transformer (defined in Sec. 3.3) to minimize the loss:

$$\begin{aligned} L &:= E_{t \in [1, T], x_0^{1:N} \sim q(x_0^{1:N}), \epsilon \sim \mathcal{N}(\mathbf{0}, \mathbf{I})} [\|\epsilon - \epsilon_\theta(x_t^{1:N}, t, c)\|^2] \\ &:= E_{t \in [1, T], x_0^{1:N} \sim q(x_0^{1:N}), \epsilon \sim \mathcal{N}(\mathbf{0}, \mathbf{I})} [\|\epsilon - \epsilon_\theta(\sqrt{\alpha_t} x_0^{1:N} \\ &\quad + \epsilon \sqrt{1 - \alpha_t}, t, c)\|^2]. \end{aligned} \quad (6)$$

3.3 Bipartite Graph Interaction Transformer

The Bipartite Graph Interaction Transformer used by BiGraphDiff is based on the original Transformer [Vaswani *et al.*, 2017]. It is composed of a text encoder, embedding and positional encoding layers, self-attention modules, cross-attention modules, a Bipartite graph module, feed-forward modules, and a final linear layer. We input $x_t^{1:N}$ and c to obtain $\epsilon_\theta(x_t, t, c)$.

Text Encoder. The text encoder is used to encode c the class label. We use a simple four layers Transformer encoder as described in [Vaswani *et al.*, 2017] that uses multi-head self-attention. To avoid training the encoder from scratch, we initialize the weight with those of CLIP [Radford *et al.*, 2021].

Motion Decoder. The motion decoder uses $x_t^{1:N}$ and the output of the text encoder to obtain $\epsilon_\theta(x_t, t, c)$. First we split $x_t^{1:N}$ into $x_{1,t}^{1:N}$ and $x_{2,t}^{1:N}$ which represent the first and second skeleton, respectively. Each skeleton passes through an

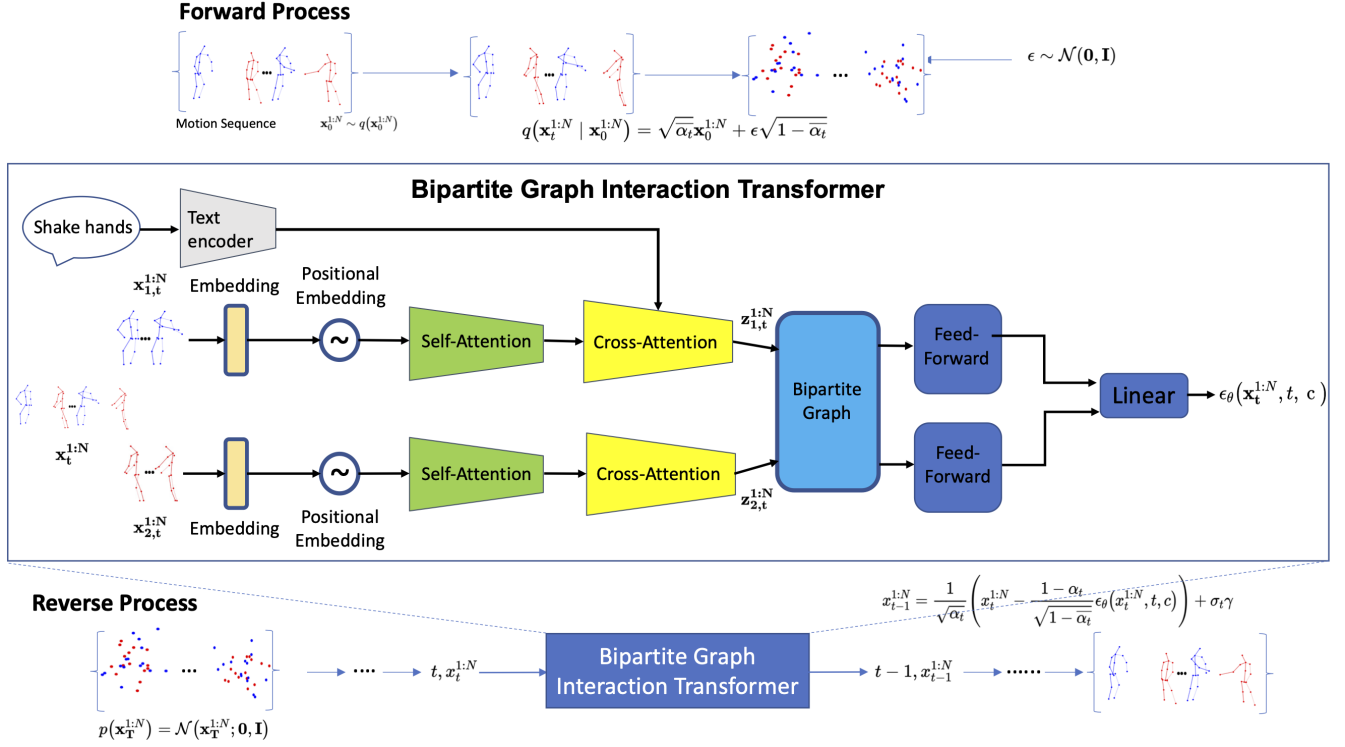


Figure 1: **BiGraphDiff overview.** Top: the forward diffusion process to add noise to the motion sequence. Middle: the proposed Bipartite Graph Interaction Transformer to learn the denoising function. Bottom reverse diffusion process to generate motion sequence from noise.

embedding layer followed by a positional encoding layer introduced by [Vaswani *et al.*, 2017] that encodes the temporal information from each frame of the sequence.

Self-Attention and Cross-Attention Then the data goes through self-attention and cross-attention layers. Attention is used to find correlations within the data and is defined as

$$\text{Attention}(\mathbf{Q}, \mathbf{K}, \mathbf{V}) = \text{softmax}\left(\frac{\mathbf{Q}\mathbf{K}^T}{\sqrt{d}}\right) \mathbf{V}, \quad (7)$$

where \mathbf{Q} , \mathbf{K} , and \mathbf{V} are the query, key, and value matrices that have the same size as $x_{1,t}^{1:N}$ and $d=k*3$ the dimension of one frame from $x_{1,t}^{1:N}$. \mathbf{Q} , \mathbf{K} , and \mathbf{V} are defined for self-attention for the first skeleton as

$$\mathbf{Q} = x_{1,t}^{1:N} \mathbf{W}_q, \quad \mathbf{K} = x_{1,t}^{1:N} \mathbf{W}_k, \quad \mathbf{V} = x_{1,t}^{1:N} \mathbf{W}_v, \quad (8)$$

and for cross-attention

$$\mathbf{Q} = x_{1,t}^{1:N} \mathbf{W}_q, \quad \mathbf{K} = c_{emb} \mathbf{W}_k, \quad \mathbf{V} = c_{emb} \mathbf{W}_v, \quad (9)$$

where \mathbf{W}_q , \mathbf{W}_k , and \mathbf{W}_v are the weight matrices for the projection and c_{emb} the text embedding from the text encoder. This type of attention is also used in the text encoder. The issue with using this attention is its complexity. Indeed the complexity is N^2d . This means that long sequences take a very long time to be processed on top of taking a lot of memory space. To solve this issue and following the similar observation from [Zhang *et al.*, 2022], we use efficient attention instead. Efficient attention was introduced by [Shen *et al.*,

2021] to have a linear complexity on attention by calculating a global feature map instead :

$$\begin{aligned} \mathbf{F} &= \text{softmax}(\mathbf{K}^T) \mathbf{V}, \\ \text{Attention} &= \text{softmax}(\mathbf{Q}) \mathbf{F}. \end{aligned} \quad (10)$$

This simple modification allows us to get a complexity of $d_h^2 N h$ for the attention with h the number of heads and d_h the dimension of each head. d_h being a fixed value and much smaller than N , the complexity is much lower than standard attention. These heads are a part of the multi-head attention, a concept introduced by [Vaswani *et al.*, 2017] where we split the inputs into smaller parts of size d_h . Each part is fed to a head that contains its own attention module. The output of all the heads is then concatenated. We use 8 heads for both self-attention and cross-attention. Each attention layer (self and cross) is followed by a stylization block. This module, introduced by [Zhang *et al.*, 2022] allows the generative process to keep track of the current diffusion timestep t improving the generation. The output of this module is added to the input of the attention through a residual connection.

Bipartite Graph. Following the self-attention and cross-attention module, both skeletons, $z_{1,t}^{1:N}$ and $z_{2,t}^{1:N}$ go through the bipartite graph module. The proposed bipartite graph aims to capture the long-range cross relations between the two skeletons $S_a = z_{1,t}^{1:N}$ and $S_b = z_{2,t}^{1:N}$ in a bipartite graph via GCNs. Each node in S_a is connected to all the nodes in S_b . Firstly, S_a and S_b are separately fed into two encoders to obtain the feature F_a and F_b , respectively.

We then reduce the dimension of F_a with the function $\varphi_a(F_a) \in \mathbb{R}^{C \times D_a}$, where C is the number of feature map channels, and D_a is the number of nodes of F_a . Meanwhile, we reduce the dimension of F_b with the function $\theta_b(F_b) = H_b^T \in \mathbb{R}^{D_b \times C}$, where D_b is the number of nodes of F_b . Next, we project F_a to a new feature V_a in a bipartite graph using the projection function H_b^T . Thus we have:

$$V_a = H_b^T \varphi_a(F_a) = \theta_b(F_b) \varphi_a(F_a), \quad (11)$$

where both functions $\theta_b(\cdot)$ and $\varphi_a(\cdot)$ are implemented using a 1×1 convolutional layer. This results in a new feature $V_a \in \mathbb{R}^{D_b \times D_a}$ in the bipartite graph, which represents the cross relations between the nodes of the skeleton F_b and the skeleton F_a .

After projection, we employ a fully connected bipartite graph with adjacency matrix $A_a \in \mathbb{R}^{D_b \times D_b}$. We then use a graph convolution to learn the long-range cross relations between the nodes from both skeletons, which can be represented as:

$$M_a = (I - A_a)V_aW_a, \quad (12)$$

where $W_a \in \mathbb{R}^{D_a \times D_a}$ denotes the trainable edge weights. We use Laplacian smoothing [Chen *et al.*, 2019; Li *et al.*, 2018] to propagate the node features over the bipartite graph. The identity matrix I can be viewed as a residual sum connection to alleviate optimization difficulties. We randomly initialize both the adjacency matrix A_a and the weights W_a and then train them by gradient descent.

After the cross-reasoning process, the new updated feature M_a is mapped back to the original coordinate space for further processing. Next, we add the result to the original feature F_a to form a residual connection, as follows:

$$\tilde{F}_a = \phi_a(H_b M_a) + F_a, \quad (13)$$

where we reuse the projection matrix H_b and apply a linear projection $\phi_a(\cdot)$ to project M_a back to the original coordinate space. Therefore, we obtain the feature \tilde{F}_a , which has the same dimension as the original one F_a .

Similarly, we can obtain the new feature \tilde{F}_b . Overall, the proposed method reasons the cross relations between feature maps of different skeletons using a bipartite graph.

Feed-Forward Network. After the bipartite graph module, the data of each skeleton goes through a feed-forward network. It is composed of linear projections, dropout, and GELU activation functions. It is followed by a stylization block to ensure that the information about the current timestep is not lost. The output is added to the input of the feed-forward network thanks to a residual connection.

Linear Transformation. The Motion decoder described above contains 8 identical layers and the input of layer m is the output of layer $m - 1$. Following those 8 layers the data of the two skeletons is concatenated and goes through a final linear projection to obtain $\epsilon_\theta(x_t, t, c)$ that we can use in our loss and to retrieve $x_{t-1}^{1:N}$.

4 Experiments

4.1 Datasets

There are few 3D motion two-persons interaction datasets. Therefore we focus on two complementary datasets. The

NTU RGB+D 120 dataset [Liu *et al.*, 2019], among its 120 classes, contains 26 classes labeled as ‘‘Mutual Actions / Two Person Interactions’’ which show two persons performing simple interaction motions. We take this 26 classes subset that we call NTU-26 and split each class randomly to obtain our training and testing set. The testing set contains 2,600 samples (100 per class) and the training set is 19,787 samples. The second dataset is DuetDance [Kundu *et al.*, 2020], which contains five classes of two persons dance motions for a total of 406 sequences. The motions are more complex than the one from NTU-26 and harder to classify, even for a human observer. The original dataset contains motions with great variations in lengths from 100 frames to more than 4,000. The average length is 483 frames with a median of 360 frames. While our model can generate very long motions it causes a problem when obtaining quantitative results and lower the quality of the generation due to the limited presence of some sequence of certain lengths. We decided to split the sequences into subsequences of 300 frames or less. This increases the number of samples to train our network with. This increased number of samples will also help the diffusion model since it needs a lot of data. This leaves us with 698 training samples and 125 test samples (25 per class randomly selected).

4.2 Implementation Details

We train our model on an NVIDIA A100 80Go GPU with PyTorch with a batch size of 128 for NTU and 64 for DuetDance. We train on NTU for 1,500 epochs and for 30,000 epochs on DuetDance.

4.3 Baselines

We compare BiGraphDiff to two methods from the state-of-the-art, i.e., MotionDiffuse [Zhang *et al.*, 2022] and ACTOR [Petrovich *et al.*, 2021]. MotionDiffuse, a recent Diffusion and Transformer based architecture, generates a single-person motion from the text. For our experiments, the code provided by the author and recommended parameters are used. Due to the similarity with our method, however, we take the same batch size and number of epochs as for our method. ACTOR, a Transformer VAE method, generates a single-person motion. We use the code provided by the authors and retrain it on our datasets. We use the recommended parameters to run the model without SMPL [Loper *et al.*, 2015] loss function. SMPL loss function is deactivated because SMPL is not available in NTU RGB+D and DuetDance datasets.

4.4 Quantitative Results

We perform the quantitative evaluation by using classification accuracy, Frechet Video Distance (FVD) score, and Multimodality. The classification accuracy is obtained using a simple Transformer encoder followed by an MLP. The classifier is trained and tested on the same set as the generative methods.

NTU-26. Table 1 shows that our method outperforms the two the-state-of-art methods in terms of average accuracy. BiGraphDiff outperforms MotionDiffuse by 7.0% and ACTOR

Table 1: Classification score on NTU-26.

Method	GT	ACTOR [Petrovich <i>et al.</i> , 2021]	MotionDiffuse [Zhang <i>et al.</i> , 2022]	BiGraphDiff
Classification Accuracy \uparrow				
Punching	76.0%	1.0%	43.0%	49.0%
Kicking	86.0%	14.0%	61.0%	86.0%
Pushing	97.0%	77.0%	86.0%	74.0%
Pat on back	88.0%	4.0%	72.0%	80.0%
Point Finger	83.0%	0.0%	52.0%	76.0%
Hugging	97.0%	59.0%	90.0%	97.0%
Giving object	91.0%	34.0%	68.0%	86.0%
Touch pocket	93.0%	35.0%	81.0%	84.0%
Shaking hands	89.0%	16.0%	80.0%	90.0%
Walking toward	93.0%	72.0%	98.0%	99.0%
Walking apart	95.0%	90.0%	90.0%	90.0%
Hit with object	44.0%	8.0%	23.0%	28.0%
Wield knife	50.0%	7.0%	31.0%	41.0%
Knock over	85.0%	4.0%	61.0%	61.0%
Grab stuff	74.0%	0.0%	57.0%	62.0%
Shoot with gun	57.0%	1.0%	46.0%	44.0%
Step on foot	89.0%	5.0%	85.0%	90.0%
High five	90.0%	4.0%	75.0%	78.0%
Cheers and drink	90.0%	16.0%	69.0%	92.0%
Carry object	96.0%	98.0%	92.0%	95.0%
Take a photo	87.0%	19.0%	63.0%	80.0%
Follow	94.0%	68.0%	90.0%	81.0%
Whisper	83.0%	0.0%	72.0%	79.0%
Exchange things	88.0%	6.0%	65.0%	78.0%
Support somebody	94.0%	100.0%	94.0%	92.0%
Rock paper scissor	91.0%	6.0%	75.0%	91.0%
Average	84.6%	30.7%	70.0%	77.0%

Table 2: FVD and Multimodality on NTU-26.

Method	FVD \downarrow	Multimodality \downarrow
ACTOR [Petrovich <i>et al.</i> , 2021]	25298.73	34.91
MotionDiffuse [Zhang <i>et al.</i> , 2022]	1292.32	14.94
BiGraphDiff	1048.13	11.28

by 46.3%. We are also very close to the accuracy of the classifier on the ground truth. This shows that the sequences generated by our method are realistic and correspond to the input class. In more detail, we can see that we outperform or equate the other methods on 22 classes out of 26. MotionDiffuse and ACTOR are both better in 2 classes. However, we can see that ACTOR results being actually better is debatable as some classes have very low accuracy, down to 0%. We can also see that the classes in which we perform the worse (i.e., “Hit with object” 28%, “Wield knife” 41%, and “Shoot with gun” 44%) are the ones where the results are also low for the ground truth. Those are classes where the main difference is the object used which is something we can not see using 3D skeleton data. Table 2 shows the FVD and multimodality results. In terms of FVD and Multimodality, our method also outperforms the two other methods indicating that our method produces sequences closer to the real data. One issue when using the NTU dataset is that it is very noisy (see the ground truth in the qualitative results). This means that it is harder to generate noiseless sequences but also that a method

that generates samples without noise might be disadvantaged in the quantitative results since they are compared with the ground truth and the classifier is trained on the noisy data.

DuetDance. Table 3 shows the classification results on the DuetDance dataset. We can see that, as on NTU-26, we have the best performance on average. The accuracy of our method is 9.6% higher than on MotionDiffuse and only 6.4% lower than on the ground truth. We can note that the accuracy for the ground truth is much lower than for NTU-26. This is due to the nature of the motion in DuetDance. The dance motions are much harder to recognize even for a human and also longer so it is not surprising that the results are worse. ACTOR, on the other only achieves results slightly higher than chance (20%) we will see in the qualitative results that on DuetDance, ACTOR does not produce any motion, we will discuss this in detail in the qualitative results. In the “jive” class, all methods only achieve chance level or lower accuracy. But the results are not so low for the ground truth with means that all methods have trouble generating motion of the “jive class”. In Table 4, we show that we outperform the other methods on both metrics meaning that the results of our method are more realistic.

4.5 Qualitative Results

NTU-26. Figure 2 shows visuals of sequences generated for the “Cheers and drinks” class. This class of motion is more complex than others because it is composed of two separate motions “cheers” and “drink”. All methods generate a proper

Table 3: Classification score on DuetDance.

Method	GT	ACTOR [Petrovich <i>et al.</i> , 2021]	MotionDiffuse [Zhang <i>et al.</i> , 2022]	BiGraphDiff
Classification Accuracy \uparrow				
Cha-cha	28.0%	36.0%	32.0%	32.0%
Jive	52.0%	16.0%	20.0%	16.0%
Rumba	56.0%	16.0%	48.0%	68.0%
Salsa	88.0%	0.0%	64.0%	76.0%
Samba	52.0%	80.0%	32.0%	52.0%
Average	55.2%	29.6%	39.2%	48.8%

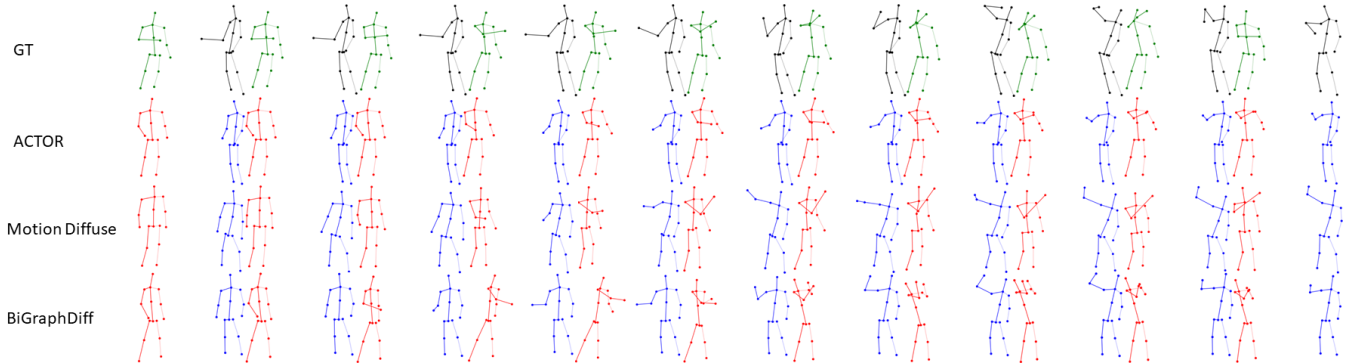


Figure 2: Examples of diverse motion generation for a given text prompt “Cheers and Drink” action from NTU.

Table 4: FVD and Multimodality on DuetDance.

Method	FVD \downarrow	Multimodality \downarrow
ACTOR [Petrovich <i>et al.</i> , 2021]	2641.08	67.79
MotionDiffuse [Zhang <i>et al.</i> , 2022]	1133.51	12.24
BiGraphDiff	997.92	4.33

motion but ACTOR shows a low intensity for “cheers” and does not really generate the “drink” motion. MotionDiffuse generates a good motion with both “cheers” and “drink” but there is some noise and the arm length grows over time. Our method generates the proper motion with the two steps and does not produce the noise that is present in the ground truth. In our case, one character drinks while grabbing the glass with one hand while the other use both hands showing the diversity in the generated motions. Overall we see that our motion is more realistic, temporally, and spatially coherent and manages well to keep the interaction coherent.

DuetDance. Figure 3 shows examples of motion generation of the “salsa” class. The dance motions are more complex and the sequences are longer than NTU-26 sequences. ACTOR does not produce motion. We believe this to be due to the great variability of motions from the same class. ACTOR converges to a mean and finds that an unmoving pair of skeletons is the best generation for its losses. We see that MotionDiffuse produces a dance motion without noise. This is because there is less noise in DuetDance than in NTU-26. Our method also generates a dance motion but is better than MotionDiffuse, we reproduce the motion of characters changing sides that is present in the ground truth and the interaction is better as the arm of both characters does not overlap.

Table 5: User study results (%).

Method	NTU-26		DuetDance	
	Q1	Q2	Q1	Q2
ACTOR [Petrovich <i>et al.</i> , 2021]	6.1	7.8	5.6	5.9
MotionDiffuse [Zhang <i>et al.</i> , 2022]	22.4	24.3	21.8	23.7
BiGraphDiff	31.6	32.7	28.5	30.1
GT	39.9	35.2	44.1	40.3

4.6 User Study

The user study compared BiGraphDiff with two leading methods (i.e., ACTOR [Petrovich *et al.*, 2021], MotionDiffuse [Zhang *et al.*, 2022]) and the ground truth sequence. For both datasets, we randomly select 20 samples for each class from the test data. For each comparison, 30 participants are asked to answer two questions, i.e., ‘Q1: Which skeleton sequence is more realistic?’, and ‘Q2: Which skeleton sequence matches the input text better?’. The numbers indicate the preference percentage of users who favor the results of the corresponding methods or the GT skeleton sequence. The results highlight the quality of the sequence generated by our method.

4.7 Ablation Study

We report ablation results in Table 6 on the NTU-26 dataset. We compare a simple two-stream Transformer (S1), a two-stream Transformer in a diffusion process (S2), a two-stream Transformer in a diffusion process with a simple GCN (S3), and finally our method with bipartite graphs (S4).

The results of S1 are extremely bad. It is explained by

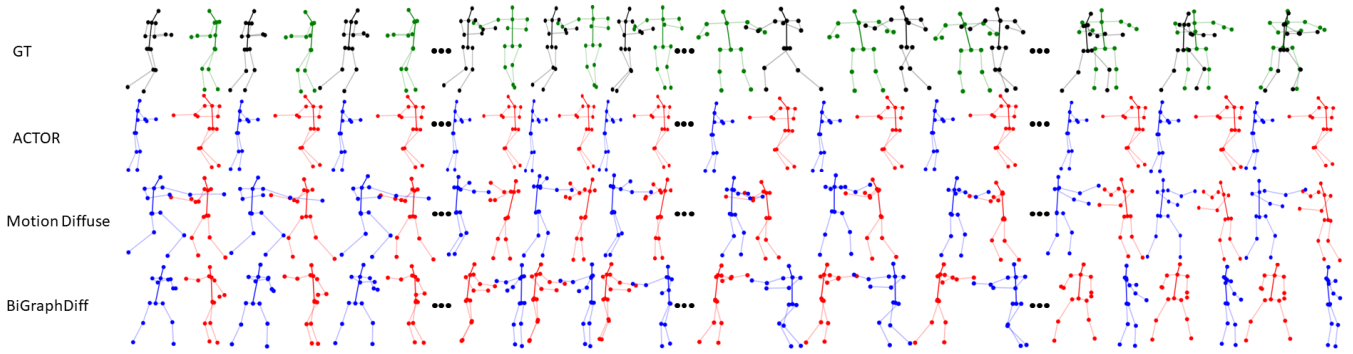


Figure 3: Examples of diverse motion generation for a given text prompt “Salsa” action from DuetDance.

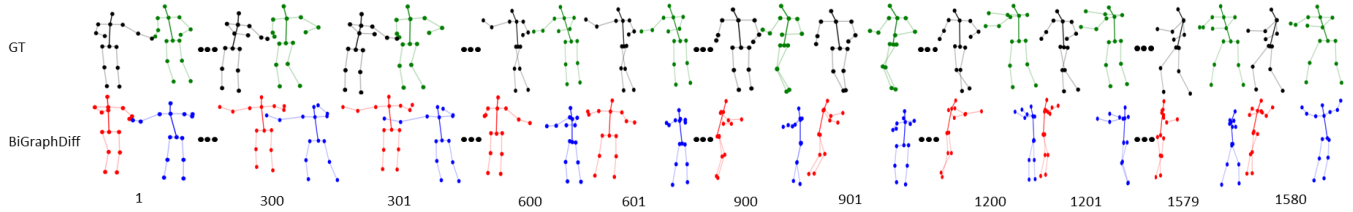


Figure 4: Example of generation of very long sequences on the “rumba” class from DuetDance. Under each skeleton the frame number.

Table 6: Ablation study on NTU.

Method	Classification↑	FVD↓
S1: Two Stream Transformer	3.9%	21215.21
S2: Two Stream Transformer + Diffusion	69.3%	1406.09
S3: S2 + Simple GCN	73.2%	1123.88
S4: S2 + Bipartite Graph	77.0%	1048.16

the fact the Transformer is a deterministic method and has a low generation diversity which explains the very high FVD. Furthermore, the noisy data from the NTU dataset makes it even harder to provide well-generated sequences. S2 provides much better results both in classification accuracy and FVD, the results are similar to the results obtained by MotionDiffuse. With S3 the simple GCN helps enhance the generation leading to better accuracy and FVD. This highlights the ability of the GCN to model more accurately the spatio-temporal dependencies from each skeleton. Adding a bipartite graph network in S4 provides a stronger increase in performance. It shows that modeling the interactions between the two skeletons is more important than trying to refine the interactions inside each skeleton like S3 did. It validates the use of the bipartite graph network in BiGraphDiff architecture.

5 Very Long Generation

Long-term motion generation plays an important role in real-world applications. Our method is able to generate longer sequences as shown in Figure 4. We train the network on the original DuetDance dataset with a maximum sequence length of 4050 frames. We use 376 samples for training and 40 (8 per class) for testing. Figure 4 shows an example of 1580 frames from the “rumba” class. We can see that we generate dance-like motion for the entire duration of the sequence.

However, it is very noticeable that we generate better motion for the first few hundred frames, we see that the motion quality around 300 frames is good but then around 600 frames we see deterioration that gradually becomes worse. This is due to the length of the sequences in the DuetDance dataset distribution which are usually not very long (average: 483 frames, median: 360 frames).

6 Conclusion, Limitations and Future Work

We introduce the first approach for 3D human motion interactions based on denoising diffusion models. Both quantitative and qualitative evaluations show that BiGraphDiff outperforms state-of-the-art methods. The proposed BiGraphDiff method generates coherent human motion sequences that are longer and more diverse than the results of previous approaches.

The proposed BiGraphDiff suffers however from the common limitations of diffusion models: the need for large datasets and the long training and testing duration. The method is also still slightly sensitive to noise in the training data and can sometimes generate deformed skeletons. This is due in part to the quality of the data used but also because we do not set any constraint related to the input data, e.g., bone length or relative position of joint for 3D skeletons. This means that BiGraphDiff can be used for tasks other than human interaction generation. As long as the input data can be split into two sets and has a temporal or positional component BiGraphDiff can be used for generation.

Acknowledgments

This project has received financial support from the CNRS through the 80—Prime program.

7 Appendix

A Evaluation Metrics Details

Classification Accuracy. To evaluate the generated sequence, we use a classifier made of a simple Transformer encoder followed by an MLP. The classifier is trained and tested on the same training and testing sets as the generative methods. We look at the percentage of correctly classified samples in each class and the average over the entire testing set.

FVD. Fréchet Video Distance (FVD) adapts the Fréchet Inception distance (FID) [Heusel *et al.*, 2017] for video sequences [Unterthiner *et al.*, 2018]. With FVD, we compute the distance between the generated data distribution and the ground truth using deep features.

$$\text{FVD} = |\mu_{gt} - \mu_{gen}|^2 + \text{tr} \left[\mathbf{C}_{gt} + \mathbf{C}_{gen} - 2(\mathbf{C}_{gt} * \mathbf{C}_{gen})^{1/2} \right], \quad (14)$$

where μ_{gt} , μ_{gen} and \mathbf{C}_{gt} and \mathbf{C}_{gen} are the means and covariance matrices of the deep features from ground truth and the generated samples respectively, $\text{tr}(\cdot)$ is the trace. We obtain the deep features from one of the last MLP layer from the classifier used to get the classification accuracy.

Multimodality. Multimodality is defined as the average of deep features distance of the samples generated by a method compared to the average deep features distance of the ground truth on a specific class. Multimodality allows us to see if the samples we generate are different from each other. It corresponds to intra-class diversity. To compute the average deep features distance we split the set of features of each class into two equal sets and compare the euclidean norm between the pairs formed by a member of each set and compute the average over the size of the subsets. The average deep features distance for multimodality is defined as follows:

$$\text{dist} = \frac{1}{cm} \sum_{j=1}^c \sum_{i=1}^m \|F_{ji}^A - F_{ji}^B\|_2, \quad (15)$$

where c is the number of classes in the dataset F_{ji}^A and F_{ji}^B the i^{th} features of the subset A and B of class j . The multimodality is then calculated as follows:

$$\text{score} = 100 \times \frac{|\text{dist}_{gt} - \text{dist}_{gen}|}{\text{dist}_{gt}}, \quad (16)$$

with dist_{gt} and dist_{gen} the deep features distance of the ground truth and of the considered method, respectively. The lower the multimodality the better, as it means that we are close to the multimodality of real data.

B Additional Qualitative Results

NTU-26. Figures 5 and 6 show visuals of sequences generated for the “High-five” and “Kicking” classes, respectively. For “High-five”, ACTOR also generates a low-intensity motion, and both characters raise their hand but do not perform a high-five. Both MotionDiffuse and our method generate a high-five but MotionDiffuse shows noise and the hands of both characters stay far from each other. The ground truth once again contains noise that is not present in our generation. For the “Kicking” class, ACTOR does not generate any

motion for either character. MotionDiffuse generates the red character as being kicked but does not generate the blue person kicking. Our method, on the other hand, generates both the kicking motion and the other character being kicked like the ground truth. In the ground truth, we can see that the leg is never fully extended during the kick. This is common for this class. The NTU-RGB+D dataset is captured using a Kinect camera and has difficulties capturing the legs due to camera positioning and occlusion during interactions. This shows the kind of noise present in the original data again. Overall we see that our motions are more realistic, temporally, and spatially coherent, and manage well to keep the interaction coherent.

C Video Results

Videos of the qualitative results presented can be found at <https://drive.google.com/drive/folders/11zW5hmWGW0csKp8XX9GwTijVCRp4j2hQ?usp=sharing> in “Videos.zip”. In “Cheer_and_drink.mp4”, “High_five.mp4”, “Kicking.mp4”, and “salsa.mp4” we show a comparison of the GT, the two state-of-the-art methods and BiGraphDiff on the four classes presented in the main paper and the supplementary material. In file “very_long_rumba.mp4”, we show the video for very long-term generation on the rumba class presented in the main paper.

D Additional animated results

At <https://drive.google.com/drive/folders/11zW5hmWGW0csKp8XX9GwTijVCRp4j2hQ?usp=sharing> in “Visuals_gif.zip” are additional animated results produced by BiGraphDiff. The visuals are in “.gif” format and can take some time to load for the longer sequences. “BiGraphDiff_NTU.zip” contains the results on the NTU-26 dataset (100 samples per class) and “BiGraphDiff_DuetDance.zip” contains the results on the DuetDance dataset (25 samples per class).

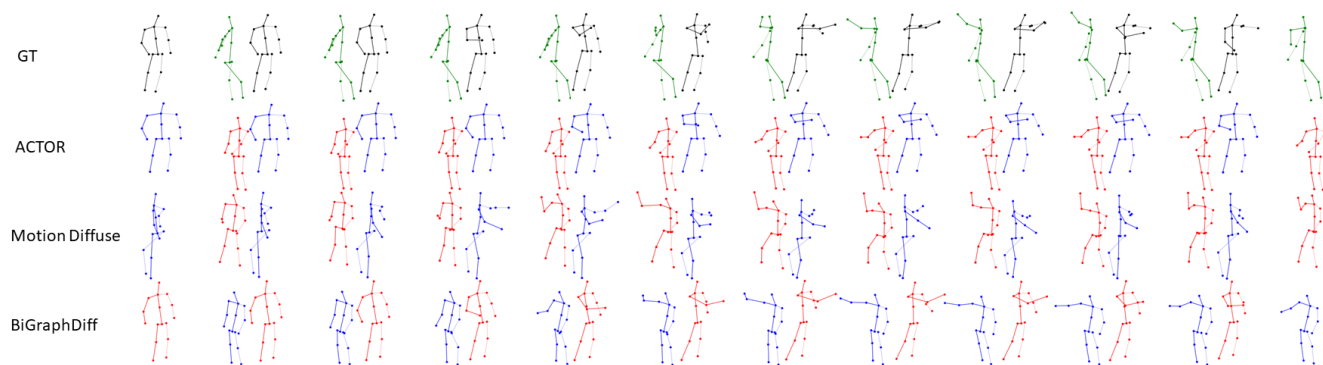


Figure 5: Examples of diverse motion generation for a given text prompt “High-five” action from NTU.

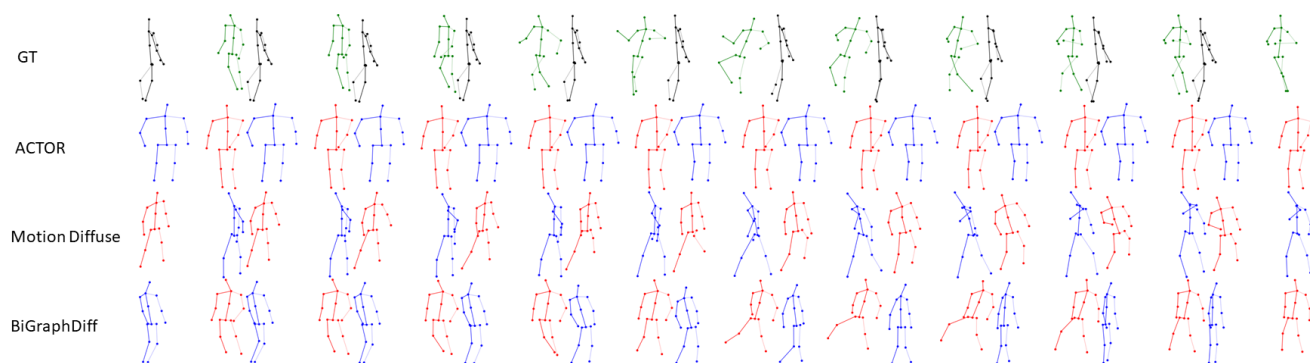


Figure 6: Examples of diverse motion generation for a given text prompt “Kicking” action from NTU.

References

- [Ahuja *et al.*, 2020] Chaitanya Ahuja, Dong Won Lee, Ryo Ishii, and Louis-Philippe Morency. No gestures left behind: Learning relationships between spoken language and freeform gestures. In *EMNLP*, 2020.
- [Alexanderson *et al.*, 2022] Simon Alexanderson, Rajmund Nagy, Jonas Beskow, and Gustav Eje Henter. Listen, denoise, action! audio-driven motion synthesis with diffusion models. *arXiv preprint arXiv:2211.09707*, 2022.
- [Baruah and Banerjee, 2020] M. Baruah and B. Banerjee. A multimodal predictive agent model for human interaction generation. In *CVPR Workshops*, 2020.
- [Chen *et al.*, 2019] Yunpeng Chen, Marcus Rohrbach, Zhicheng Yan, Yan Shuicheng, Jiashi Feng, and Yannis Kalantidis. Graph-based global reasoning networks. In *CVPR*, 2019.
- [Cui *et al.*, 2020] Qiongjie Cui, Huaijiang Sun, and Fei Yang. Learning dynamic relationships for 3D human motion prediction. In *CVPR*, 2020.
- [Dabral *et al.*, 2022] Rishabh Dabral, Muhammad Hamza Mughal, Vladislav Golyanik, and Christian Theobalt. Mo-fusion: A framework for denoising-diffusion-based motion synthesis, 2022.
- [Guo *et al.*, 2022] Chuan Guo, Xinxin Zuo, Sen Wang, and Li Cheng. TM2T: stochastic and tokenized modeling for the reciprocal generation of 3d human motions and texts. In *Computer Vision - ECCV 2022 - 17th European Conference, Tel Aviv, Israel, October 23-27, 2022, Proceedings, Part XXXV*, pages 580–597, 2022.
- [Habibie *et al.*, 2021] Ikhsanul Habibie, Weipeng Xu, Dushyant Mehta, Lingjie Liu, Hans-Peter Seidel, Gerard Pons-Moll, Mohamed Elgharib, and Christian Theobalt. Learning speech-driven 3d conversational gestures from video. In *ACM International Conference on Intelligent Virtual Agents (IVA)*, 2021.
- [Harvey *et al.*, 2022] William Harvey, Saeid Naderiparizi, Vaden Masrani, Christian Weilbach, and Frank Wood. Flexible diffusion modeling of long videos. *arXiv preprint arXiv:2205.11495*, 2022.
- [Heusel *et al.*, 2017] Martin Heusel, Hubert Ramsauer, Thomas Unterthiner, Bernhard Nessler, and Sepp Hochreiter. Gans trained by a two time-scale update rule converge to a local nash equilibrium. In *NeurIPS*, 2017.
- [Ho *et al.*, 2020a] Jonathan Ho, Ajay Jain, and Pieter Abbeel. Denoising diffusion probabilistic models. *arXiv preprint arxiv:2006.11239*, 2020.
- [Ho *et al.*, 2020b] Jonathan Ho, Ajay Jain, and Pieter Abbeel. Denoising diffusion probabilistic models. In H. Larochelle, M. Ranzato, R. Hadsell, M.F. Balcan, and H. Lin, editors, *Advances in Neural Information Processing Systems*, volume 33, pages 6840–6851. Curran Associates, Inc., 2020.
- [Hoogeboom *et al.*, 2022] Emiel Hoogeboom, Víctor Garcia Satorras, Clément Vignac, and Max Welling. Equivariant diffusion for molecule generation in 3D. In Kamalika Chaudhuri, Stefanie Jegelka, Le Song, Csaba Szepesvari, Gang Niu, and Sivan Sabato, editors, *Proceedings of the 39th International Conference on Machine Learning*, volume 162 of *Proceedings of Machine Learning Research*, pages 8867–8887. PMLR, 17–23 Jul 2022.
- [Kundu *et al.*, 2020] Jogendra Kundu, Himanshu Buckchash, Priyanka Mandikal, Rahul M V, Anirudh Jamkhandi, and R. Babu. Cross-conditioned recurrent networks for long-term synthesis of inter-person human motion interactions. In *WACV*, 2020.
- [Li *et al.*, 2018] Qimai Li, Zhichao Han, and Xiao-Ming Wu. Deeper insights into graph convolutional networks for semi-supervised learning. In *AAAI*, 2018.
- [Liu *et al.*, 2019] Jun Liu, Amir Shahroudy, Mauricio Perez, Gang Wang, Ling-Yu Duan, and Alex Kot. Ntu rgb+d 120: A large-scale benchmark for 3d human activity understanding. *IEEE Transactions on Pattern Analysis and Machine Intelligence*, pages 1–18, 2019.
- [Loper *et al.*, 2015] Matthew Loper, Naureen Mahmood, Javier Romero, Gerard Pons-Moll, and Michael J. Black. SMPL: A skinned multi-person linear model. *ACM Trans. Graphics (Proc. SIGGRAPH Asia)*, 34(6):248:1–248:16, October 2015.
- [Lucas *et al.*, 2022] Thomas Lucas, Fabien Baradel, Philippe Weinzaepfel, and Grégory Rogez. Posegpt: Quantization-

- based 3d human motion generation and forecasting. In *European Conference on Computer Vision (ECCV)*, 2022.
- [Martinez *et al.*, 2017] Julieta Martinez, Michael J. Black, and Javier Romero. On human motion prediction using recurrent neural networks. In *CVPR*, 2017.
- [Petrovich *et al.*, 2021] Mathis Petrovich, Michael J. Black, and Gül Varol. Action-conditioned 3D human motion synthesis with transformer VAE. In *International Conference on Computer Vision (ICCV)*, 2021.
- [Radford *et al.*, 2021] Alec Radford, Jong Wook Kim, Chris Hallacy, Aditya Ramesh, Gabriel Goh, Sandhini Agarwal, Girish Sastry, Amanda Askell, Pamela Mishkin, Jack Clark, et al. Learning transferable visual models from natural language supervision. In *International Conference on Machine Learning*, pages 8748–8763. PMLR, 2021.
- [Saharia *et al.*, 2022] Chitwan Saharia, William Chan, Saurabh Saxena, Lala Li, Jay Whang, Emily Denton, Seyed Kamyar Seyed Ghasemipour, Burcu Karagol Ayan, S Sara Mahdavi, Rapha Gontijo Lopes, et al. Photorealistic text-to-image diffusion models with deep language understanding. *arXiv preprint arXiv:2205.11487*, 2022.
- [Shen *et al.*, 2021] Zhuoran Shen, Mingyuan Zhang, Haiyu Zhao, Shuai Yi, and Hongsheng Li. Efficient attention: Attention with linear complexities. In *Proceedings of the IEEE/CVF winter conference on applications of computer vision*, pages 3531–3539, 2021.
- [Sofianos *et al.*, 2021] Theodoros Sofianos, Alessio Sampieri, Luca Franco, and Fabio Galasso. Space-time-separable graph convolutional network for pose forecasting. In *Proceedings of the IEEE/CVF International Conference on Computer Vision (ICCV)*, pages 11209–11218, October 2021.
- [Sohl-Dickstein *et al.*, 2015] Jascha Sohl-Dickstein, Eric Weiss, Niru Maheswaranathan, and Surya Ganguli. Deep unsupervised learning using nonequilibrium thermodynamics. In Francis Bach and David Blei, editors, *Proceedings of the 32nd International Conference on Machine Learning*, volume 37 of *Proceedings of Machine Learning Research*, pages 2256–2265, Lille, France, 07–09 Jul 2015. PMLR.
- [Tang *et al.*, 2020] Hao Tang, Song Bai, Philip H. S. Torr, and Nicu Sebe. Bipartite graph reasoning gans for person image generation. In *31st British Machine Vision Conference 2020, BMVC 2020, Virtual Event, UK, September 7-10, 2020*. BMVA Press, 2020.
- [Tseng *et al.*, 2022] Jonathan Tseng, Rodrigo Castellon, and C. Karen Liu. EDGE: editable dance generation from music. *CoRR*, abs/2211.10658, 2022.
- [Unterthiner *et al.*, 2018] Thomas Unterthiner, Sjoerd van Steenkiste, Karol Kurach, Raphael Marinier, Marcin Michalski, and Sylvain Gelly. Towards accurate generative models of video: A new metric & challenges. *arXiv preprint arXiv:1812.01717*, 2018.
- [Vaswani *et al.*, 2017] Ashish Vaswani, Noam Shazeer, Niki Parmar, Jakob Uszkoreit, Llion Jones, Aidan N Gomez, Lukasz Kaiser, and Illia Polosukhin. Attention is all you need. In *NeurIPS*, 2017.
- [Yin *et al.*, 2021] Wenjie Yin, Hang Yin, Danica Kragic, and Mårten Björkman. Graph-based normalizing flow for human motion generation and reconstruction, 2021.
- [Zhang *et al.*, 2022] Mingyuan Zhang, Zhongang Cai, Liang Pan, Fangzhou Hong, Xinying Guo, Lei Yang, and Ziwei Liu. Motiondiffuse: Text-driven human motion generation with diffusion model. *CoRR*, abs/2208.15001, 2022.